NANO LETTERS

2005
Vol. 5, No. 7
1371−1377

The Role of Metal Nanoparticles in Remote Release of Encapsulated Materials

Andre G. Skirtach,*,† Christophe Dejugnat,† Dieter Braun,‡ Andrei S. Susha,§ Andrey L. Rogach,§ Wolfgang J. Parak,‡ Helmuth Möhwald,† and Gleb B. Sukhorukov†,||

Max-Planck Institute of Colloids and Interfaces, Golm/Potsdam, D-14424, Germany, Center for Nanoscience and Photonics and Optoelectronics Group, Physics Department, Ludwig-Maximilians Universität of München, Amalienstr. 54, Munich, D-80799, Germany, and IRC/Department of Materials, Queen Mary University of London, Mile End Road, E1 4NS, London, U.K.

Received April 14, 2005; Revised Manuscript Received May 27, 2005

ABSTRACT

Laser mediated remote release of encapsulated fluorescently labeled polymers from nanoengineered polyelectrolyte multilayer capsules containing gold sulfide core/gold shell nanoparticles in their walls is observed in real time on a single capsule level. We have developed a method for measuring the temperature increase and have quantitatively investigated the influence of absorption, size, and surface density of metal nanoparticles using an analytical model. Experimental measurements and numerical simulations agree with the model. The treatment presented in this work is of general nature, and it is applicable to any system where nanoparticles are used as absorbing centers. Potential biomedical applications are highlighted.

Increasing interest in research on polyelectrolyte multilayers (PEMs) is stimulated by potential applications of this technology in the area of drug delivery.[1] Microcapsules are fabricated by the layer-by-layer[2] (LbL) technique through the alternate adsorption of oppositely charged polyelectrolytes[3] on various colloidal templates. Subsequently, the core is dissolved[2,4] and the remaining shells serve as capsules for materials such as polymers, enzymes, catalysts, etc. The uniqueness of such microcontainers is that they allow for tailoring the composition of their walls including incorporation of metal nanoparticles. This makes them suitable as potential delivery vesicles, including, as was shown recently, applicability for delivery of chemicals into cancer cells,[5] where the role of the microcapsules is not only to control the surface chemistry but also to protect the encapsulated material during its delivery. The ability to remotely release the encapsulated material at the site of interest is important in the drug delivery area.[6] With laser technology, the method relies on making the walls of the capsules sensitive to light by doping them with metal nanoparticles or organic dyes.[7,8] Upon laser light illumination they absorb laser energy and disrupt the local environment, thus increasing the permeability of the capsule walls. Release experiments have been done in the past with volume solutions of microgels[9] and capsules.[10] To date, however, no data have been reported on monitoring the real time release of encapsulated materials on a single capsule level, and no analysis of parameters affecting the remote release has been presented. The goals of this work are threefold: first, to investigate the remote release of encapsulated fluorescently labeled polymer in real time in order to demonstrate that the polymer leaves the interior of the capsules on a single capsule level; second, to develop a quantitative analysis of the influence of the properties of metal nanoparticles including absorption, size, and surface density on the release mechanism; and third, to develop a method for measuring the temperature increase in the vicinity of capsules for estimating the efficiency of nanoparticles as absorbing centers for remote release. Quantitative analysis was performed using an analytical model introduced to account for the temperature increase in the vicinity of the capsules during laser light illumination. The temperature rise during laser illumination was both measured experimentally and simulated numerically. The remote release experiments and temperature measurements were made using laser diodes with wavelengths located in the biologically friendly near-infrared part of the spectrum.

Recently, we have proposed a novel method for remote release of encapsulated materials based on real-time monitoring of the capsules under laser light illumination.[8] It allows

* Corresponding author. E-mail: andre.skirtach@mpikg-golm.mpg.de
† Max-Planck Institute of Colloids and Interfaces.
‡ Center for Nanoscience, Ludwig-Maximilians Universität of München.
§ Photonics and Optoelectronics Group, Ludwig-Maximilians Universität of München.
|| Queen Mary University of London.

10.1021/nl050693n CCC: $30.25
Published on Web 06/25/2005

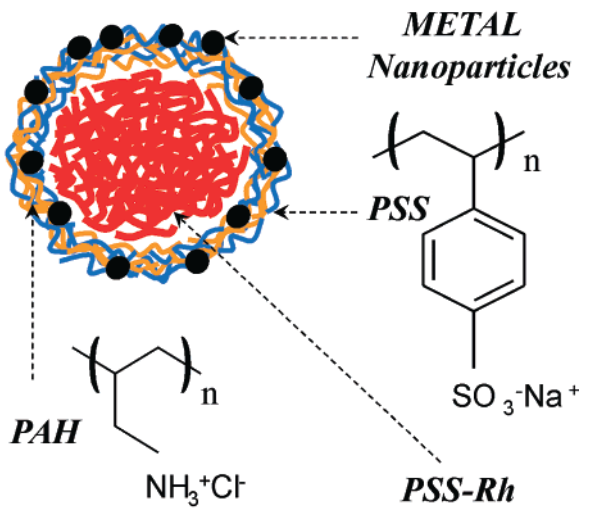

Figure 1. Schematic of a polyelectrolyte multilayer capsule with encapsulated rhodamine labeled polystyrenesulfonate polymer (PSS−Rh). Polyelectrolyte multilayer walls of capsules consist of polysterenesulfonate (PSS) and polyallylamine hydrochloride (PAH) polymers and metal nanoparticles.

for investigation of the release properties by individually addressing each capsule. The earlier work with silver nanoparticles was performed on MF (melamine formaldehyde) cores.[11] It was found that these cores leave a sponge-like matrix inside the capsules due to remaining MF oligomers.[12] Therefore, the remote release experiments with such capsules could be ambiguous. To overcome this obstacle we have used PS (polystyrene) cores that were shown suitable for fabrication of genuinely hollow capsules.[13] Briefly, coating with polyelectrolyte multilayers was done using a 10% suspension of PS latexes in water. In this work we have used cores with diameters of 5 or 10 μm. The particles were mixed with polyallylamine hydrochloride (PAH) in 0.5 M NaCl aqueous solution, and coating with one PAH layer reversed their charge from negative to positive. They were further coated with a polystyrenesulfonate (PSS) layer in a similar manner,[2] including a layer of metal nanoparticles. The influence of adsorption conditions including pH and ionic strengths was reported previously.[14−16] Hollow capsules were obtained by dissolution of the PS cores in tetrahydrofuran (THF). Hollow $(PAH/PSS)_n$ capsules containing metal nanoparticles in their walls were filled with rhodamine-labeled PSS (PSS−Rh)[17] by pH-induced encapsulation. The schematic of a filled capsule is presented in Figure 1. We note that effective encapsulation and release can be achieved with pH sensitive PEM.[18] Here, for encapsulation of the polymers we have used the property of the capsules to increase the permeability of the walls[19] at pH values above 11.5.

Important constituents of polyelectrolyte multilayers influencing their interaction with laser light are metal nanoparticles. Substantial research on metal nanoparticles was performed in recent years including attachment of DNA to gold nanoparticles,[20] functionalization of nanoparticles,[21] comprehensive studies of gold nanoparticles on planar PEMs,[22] and their interactions in PEM layers.[23] It also includes the investigation of gold nanoparticles on PEM capsules[24] and in polymer matrix,[25] synthesis of silver

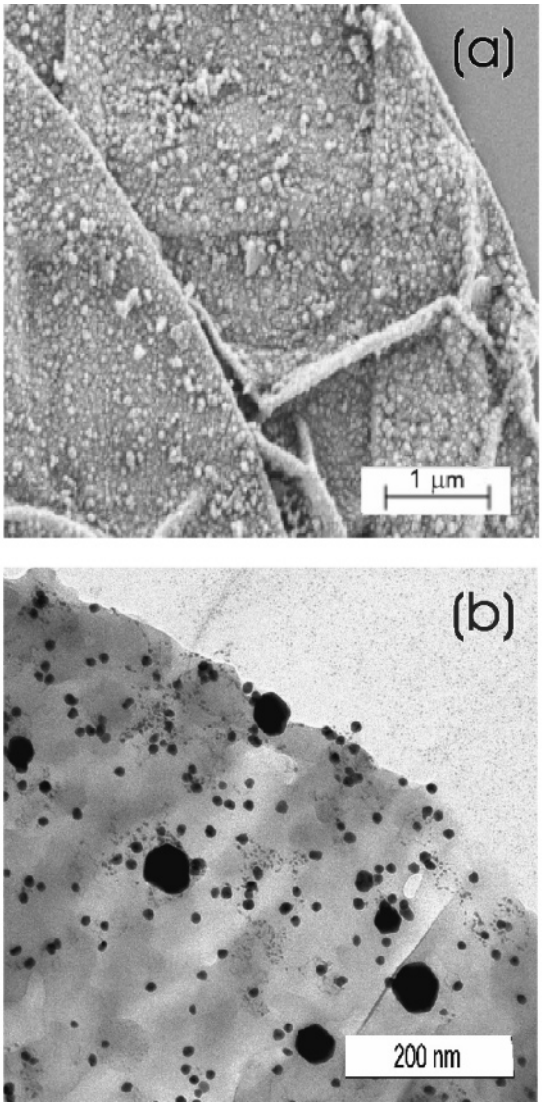

Figure 2. (a) SEM image of a capsule containing gold sulfide core/gold shell nanoparticles, (b) TEM image of a similar capsule showing two types of nonaggregated gold nanoparticles with sizes around 10 nm and gold sulfide core/gold shell nanoparticles with sizes 20 to 50 nm.

nanoparticles on capsules,[11] and silver and palladium nanoparticles on capsules.[26] In this work we have investigated the release and parameters affecting the release with capsules containing gold sulfide core/gold shell nanoparticles possessing a plasmonic absorption band in the near-infrared part of the spectrum.[7] In our case it was possible to vary the absorption in the range of 650−1000 nm by changing the synthetic conditions of reaction. The nanoparticles were synthesized in water analogous to the previously described method[27] using a two-step reaction of Na_2S with $HAuCl_4$. We would like to note that interpretation of the final products of this reaction[27−29] is the subject of continuing research.[30−32] Experimental data on single-particle measurements[30] indicated that the core−shell 20−50 nm nanoparticles are responsible for increased absorption in the near-infrared part of the spectrum. TEM image, Figure 2, indicates that products of the reaction consist of two types of nanoparticles: those with sizes around 10 nm, ascribed to pure gold

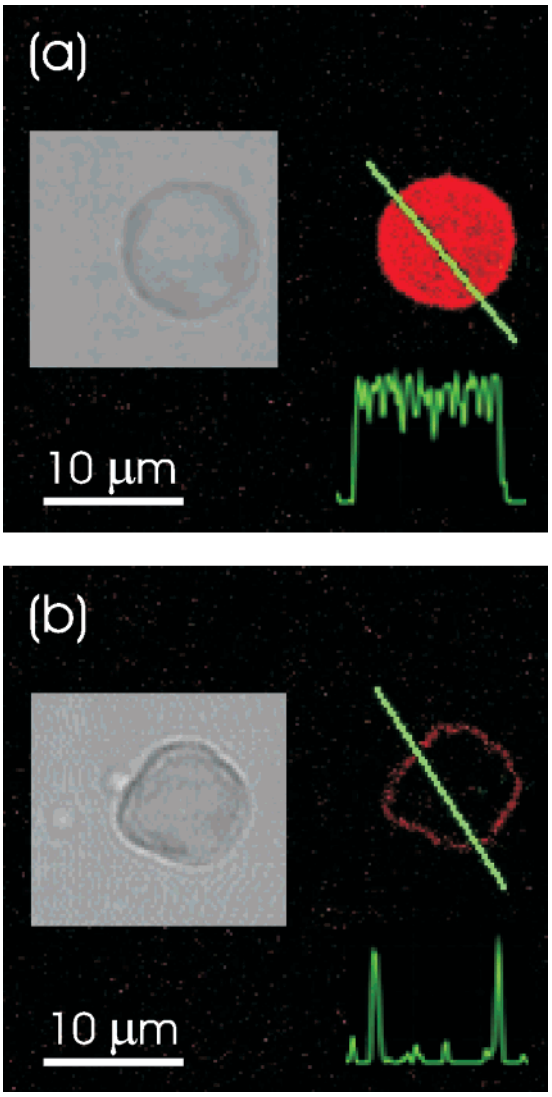

Figure 3. Confocal microscope images demonstrating remote release of encapsulated rhodamine-labeled PSS polymers from a polyelectrolyte multilayer capsule containing gold sulfide core/gold shell nanoparticles in its walls. Fluorescence intensity profiles along the line through the capsule show that it is filled with fluorescent polymers before (a) and empty after (b) laser illumination. After the release of encapsulated polymers, the leftover fluorescent intensity is observed only in the walls of the capsule, (b). Insets show black and white transmission microscope images of the same capsule. Incident intensity of laser diode operating at 830 nm was set at 50 mW.

nanoparticles, and those between 20 and 50 nm, ascribed to gold sulfide core/gold shell nanoparticles. Figures 2a and 2b present both types of nonaggregated nanoparticles incorporated in polyelectrolyte multilayer walls.

Figure 3 presents images of the release of encapsulated polymer from a single capsule containing core−shell nanoparticles in its wall. A capsule filled with rhodamine-labeled PSS could be transferred between a confocal microscope and an optical setup similar to that reported in reference 8. A modification was added to equip such a setup with fluorescence imaging. The capsule was first located on the confocal microscope and had a uniform distribution of fluorescent intensity inside, Figure 3a. The transmission microscope image of this capsule before interaction with laser light reveals its round shape, inset to Figure 3a. Consequently, the microscope coverslip containing the sample was positioned in the optical setup, and the same capsule was found again using the markings on the microscope slide. The laser was then switched on to illuminate the capsule. The real time monitoring of the release revealed that the fluorescent material instantaneously left the interior of the capsule upon exposing the whole capsule to the laser beam as shown in the movie available as Supporting Information. Then the same capsule was immediately found with the confocal microscope, Figure 3b. The transmission microscope image presented in the inset to Figure 3b demonstrates that after the release of encapsulated polymers the capsule was slightly deformed but not broken or destroyed. The leftover fluorescent trace in the rim of the capsule, Figure 3b, is an indication that some polymer remained in the capsule walls due to electrostatic interaction with polyelectrolyte multilayers. Since there is no fluorescent polymer present inside the capsule, as seen from the confocal microscope image in Figure 3b, it can be concluded that encapsulated polymer was released. Control experiments were made in which a capsule containing no gold nanoparticles was illuminated by the laser; no loss of fluorescence was observed then.

It was previously stated that the mechanism for remote release of encapsulated materials is the conversion of light into thermal energy by metal nanoparticles. To further understand the mechanism of the interaction of laser light with capsules containing metal nanoparticles, we introduce a model that accounts for the influence of absorption, size, and concentration of nanoparticles. This model establishes relationship between the temperature increase and the amount of absorbed energy. The temperature distribution around a heating sphere was obtained previously.[33] The temperature change dT between the laser switched-on and -off states at a certain distance r_i from a heating center or nanoparticle with the average radius r_0 can be written as follows:

$$\frac{\mathrm{d}T(r_i)}{\mathrm{d}E} = \frac{r_0^3}{r_i} \tag{1}$$

where $E = A/(3K)$, A is the heating rate per unit volume per unit time, and K is the thermal conductivity of the surrounding medium. The values for E can be calculated since the rate A is proportional to the incident power density and absorption.[34] We note that such an analysis can be applied to interactions of metal nanoparticles with any external field. Equation 1 reveals that temperature depends reciprocally on r_i which, under the assumption of uniform distribution of nanoparticles, can be expressed through the density of nanoparticles or surface filling factor F_S. F_S is defined as the ratio of the sum of all cross sections of n metal nanoparticles per one capsule, s_i, to the surface area of one capsule, S_C:

$$F_S = \frac{\sum_i^n s_i}{S_C} = \frac{n r_0^2}{4R_0^2} \tag{2}$$

where R_0 is the radius of a microcapsule. $F_S = 1$ corresponds to complete coverage of capsules with metal nanoparticles. The temperature decreases quickly with distance,[35] and therefore it is accurate, particularly for low values of F_S, to express the contribution only from the nearest neighbors. The average distance between nanoparticles can be expressed as follows:

$$\langle d \rangle = r_0 \frac{2}{\sqrt{F_S}} \tag{3}$$

Then eq 1 can be written in the following form:

$$\frac{dT}{dE} \cong r_0^2 \sqrt{F_S} \tag{4}$$

The significance of eq 4 is that it links the rate of temperature increase as a function of heating energy or intensity, which is a measurable quantity, with material parameters of the metal nanoparticles. However, this model is applicable for a system containing only monodisperse nanoparticles. We further consider a system comprising two types of nanoparticles of different sizes. Both smaller and larger nanoparticles would have their own absorption, radius, and surface filling factors. Equation 4 can then be extended to take into consideration the contributions of these two populations of nanoparticles:

$$\frac{dT}{dE} \cong \left(r_0^{(1)^2} \sqrt{F_S^{(1)}} + \gamma \, r_0^{(2)^2} \sqrt{F_S^{(2)}} \right) \tag{5}$$

where each term with indexes 1 and 2 refers to the nanoparticles with smaller and larger sizes, respectively. In eq 5 $E = E_1 = A_1/(3K_1)$, and $\gamma = (\alpha_2 K_1(1 - R_2))/(\alpha_1 K_2(1 - R_1)) \approx \alpha_2/\alpha_1$ if the surrounding medium is unchanged, K_i and R_i are the thermal conductivity of the medium and reflectivity, respectively, and α_i is the absorption coefficient for the smaller (i=1) and larger (i=2) nanoparticles. It can be noticed that the model, which takes into considerations the contributions from two types of nanoparticles (eq 5), is a more general case that is reduced to the simpler case represented by eq 4 when no second type of nanoparticles is present ($F_S^{(2)} = 0$ in eq 5). The expression for temperature dependence of capsules with only one type of nanoparticles (eq 4) does not explicitly have the absorption coefficient of metal nanoparticles. However, E is a function of the heating rate A, which depends on absorption. The higher absorption coefficient results in more absorption of energy leading to higher temperatures. In the case of the system of two types of nanoparticles, the coefficient γ reflects the influence of the larger nanoparticles relative to that from the smaller nanoparticles. Furthermore, the dependence of the temperature increase rate on the size of nanoparticles is quadratic, eq 4 and eq 5. This dependence is of particular interest for the system with two types of nanoparticles since the quadratic dependence on r_0 makes the influence of larger nanoparticles even more pronounced, eq 5. Indeed, the second term of the right-hand side of eq 5 is proportional to the ratio of absorption coefficients γ and r_0 in power of two. That should lead to higher temperature increase rates for nanoparticles with larger size and enhanced absorption. The analytical model presented here can be tested experimentally and applied for analyzing nanoparticles by measuring the temperature increase ΔT around capsules during laser illumination.

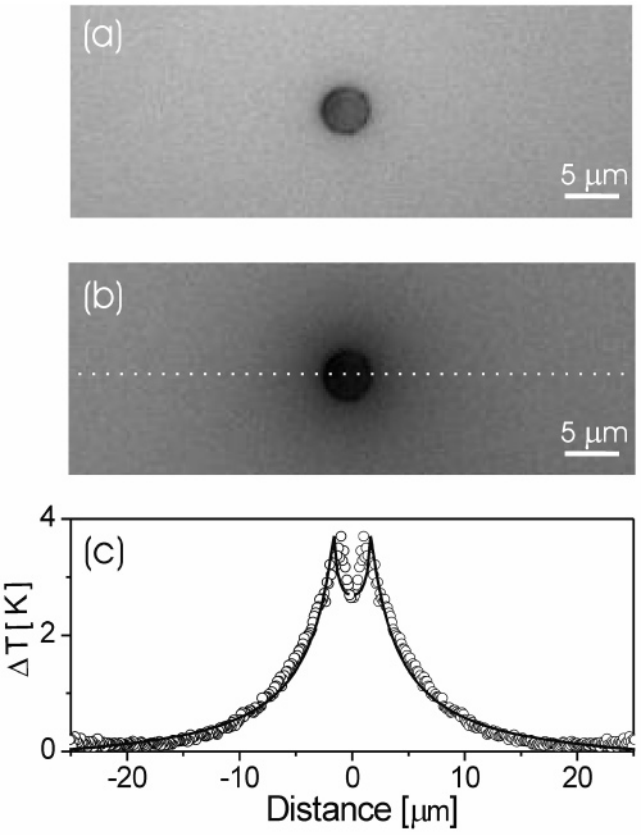

Figure 4. (a) Typical image of a hollow capsule containing gold sulfide core/gold shell nanoparticles in its walls is shown immersed in a fluorescent dye solution without laser light. (b) When laser is switched on, the temperature around the capsule increases and fluorescence of the dye solution around the capsule becomes darker. (c) Experimentally measured data for temperature change ΔT (hollow dots), extracted along the dotted line in (b), are shown together with simulated (solid line) temperature distribution induced by 980 nm laser diode operated at 25 mW. Zero coordinate is located at the center of the capsule.

We have developed a method for measuring the temperature increase at the surface of capsules during laser light illumination based on the previously reported technique.[36,37] This approach is new since all previously existing optical probes of temperature were applicable only for nonaqueous solutions. The method is based on measuring the fluorescent intensity change around a hollow (unfilled) capsule immersed in a pH sensitive dye (BCECF, Molecular Probes) in a TRIS solution. When metal nanoparticles incorporated in the walls of the capsule are heated, the solution around it becomes less fluorescent or darker. A typical measurement of the temperature distribution for a capsule containing gold sulfide core/gold shell nanoparticles is presented in Figure 4. The darkening around the capsule corresponds to an increased

temperature, Figure 4b, compared to that when no laser light is present, Figure 4a. It can be seen from Figure 4b that the fluorescence of the dye solution around the capsule is darker compared to that at a larger distance from the capsule. Since the fluorescence is measured averaged in the 20 μm thick measurement chamber the initial evaluations of the temperature give the cross-chamber average values. However, we can reliably infer the temperature at the surface of the capsules with a 3-D finite element thermal simulation (FEMLab, Comsol). The temperature at the surface of the capsules was obtained by numerical modeling in two steps. Initially, the cross-chamber volume averaged data were obtained numerically, solid line in Figure 4c. Figure 4c shows that the cross-chamber average values of the simulation matches well the experimental cross-chamber average values (hollow dots) extracted from Figure 4b along the dotted line. The next and final step in obtaining the surface temperature involved numerical simulation of the temperature distribution across 20 μm thick measurement chamber. Temperature calibration of the dye was performed in a temperature-controlled fluorometer,[38] and all temperature measurements were conducted with hollow capsules to avoid the fluorescence from the encapsulated polymers.

Analysis of the temperature increase during laser light illumination can be used for the estimation of the efficiency of metal nanoparticles as light absorbing centers. More efficient nanoparticles require lesser energy for release of encapsulated materials. The capsules with gold sulfide core-gold shell nanoparticles (Figure 2) used for release of encapsulated materials can be analyzed using the model with two types of nanoparticles, eq 5. However, a simpler system with only one type of gold nanoparticles can be used to test the simplified model with only one type of nanoparticles, eq 4. For these experiments we used gold nanoparticles prepared according to the previously reported method.[39] It can be seen from Figure 5 that these nanoparticles are not monodisperse (5 to 10 nm) but their polydispersity is relatively small compared to that of gold sulfide core/gold shell nanoparticles. The size of these gold nanoparticles can be approximated by the average value but the surface filling factor F_S can be varied. For example, F_S equals to 0.2 for the capsule presented in Figure 5a, while $F_S = 0.4$ for that in Figure 5b. F_S is adjusted by changing the concentration of nanoparticles while keeping the concentration of the capsules unchanged. Figures 5a and 5b show that although the distribution of metal nanoparticles is nonuniform, it can be varied to a large extent. The absorption spectrum, Figure 6a, reveals that these nanoparticles possess only the plasmonic absorption peak[40] around 520 nm. The measured temperature increase rates for the capsules with these gold nanoparticles for $F_S = 0.2$ and 0.4 are shown in Figure 6, samples Au I and Au II, respectively. The slopes of the graphs of the dependence of ΔT on ΔE in Figure 6b are the measures of the rates of the temperature increase. Comparing the data for capsules containing gold nanoparticles with $F_S = 0.2$ and 0.4 (Figure 6b, hollow and solid squares respectively), which are only different by their concentration, it can be seen that the increase in the surface density F_S by the factor of 2 results in the increase of the slope by the factor 1.58, which is close to $\sqrt{2} \approx 1.41$ predicted by the model. Direct comparison of samples, particularly with different nanoparticles, albeit providing valuable qualitative estimation of the influence of absorption and size, is not as rigorous. However, it is possible to estimate the influence of the size of nanoparticles by comparing the two samples containing gold sulfide core-gold shell nanoparticles. As it was already mentioned above, both of these two samples are composed of the two types of nanoparticles, the smaller and larger nanoparticles with sizes around 10 nm and 20−50 nm, respectively. Microcapsules containing gold sulfide core/gold shell nanoparticles without a pronounced peak in the near-infrared part of the spectrum, referred to as Au−CS, I (hollow circles in Figure 6b), had a low filling factor, $F_S = F_S^{(1)} + F_S^{(2)} \approx 0.05$. The temperature increase rate for these capsules was lower than that for those containing gold sulfide core/gold shell nanoparticles referred to as Au−CS,

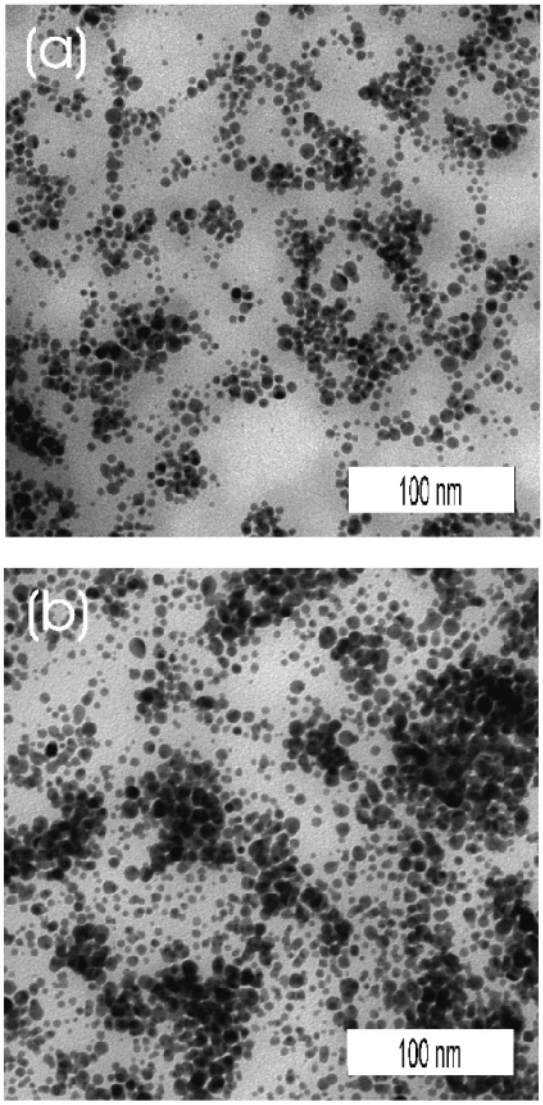

Figure 5. TEM images of capsules containing gold nanoparticles (with sizes 5 to 10 nm) in their walls with $F_S = 0.2$ (a) and $F_S = 0.4$ (b). F_S was calculated based on concentration of gold nanoparticles, measured by UV−vis spectrometer, and from TEM measurements.

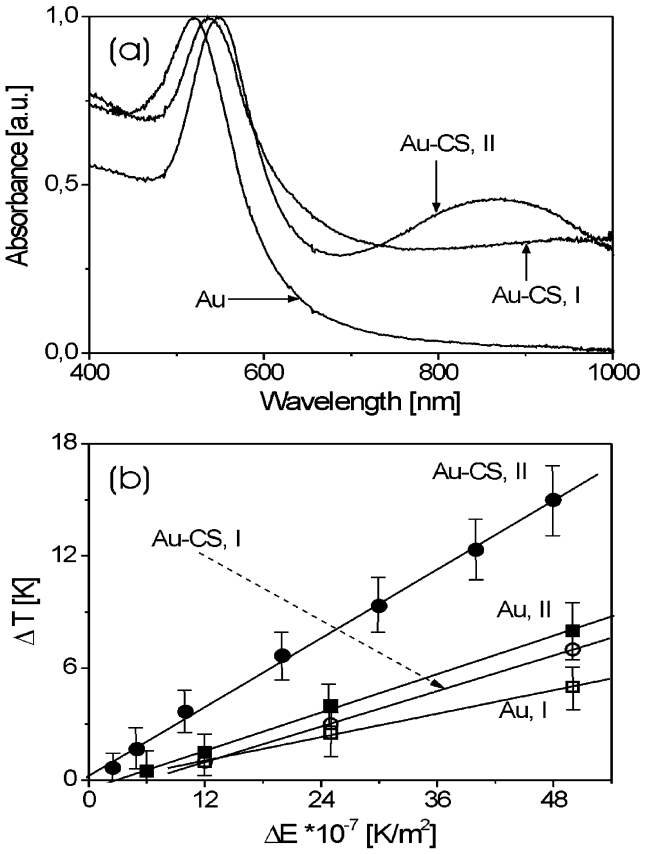

Figure 6. (a) Absorption spectra of the metal nanoparticles used in the experiments. The spectra are normalized to the peak around 530 nm. (b) The measured rates of the temperature increase at the surface of the capsules ΔT as a function of ΔE for the samples with absorption spectra presented in (a). Au−CS, I and Au−CS, II are the samples containing gold sulfide core/gold shell nanoparticles, $F_S = 0.05$ and $F_S = 0.18$, respectively. Au, I and Au, II are the samples with gold nanoparticles, $F_S = 0.2$ and $F_S = 0.4$, respectively. ΔE was calculated using the data for the incident power density, absorption and thermal conductivity.

II nanoparticles (solid circles in Figure 6b). The surface filling factor F_S for the capsules Au−CS, II was 0.18. The increase in the temperature increase rate is attributed both to larger surface filling factor F_S and also to higher absorption in the near-infrared part of the spectrum. Figure 6a shows the absorption spectra for these two samples; a broad plasmonic peak around 880 nm can be clearly seen for Au−CS, II nanoparticles. In both of the samples with gold sulfide core/gold shell nanoparticles, F_S was lower than that for the capsules with gold nanoparticles while the temperature increase is comparable or higher. This leads to a conclusion that gold sulfide core/gold shell nanoparticles are more efficient energy absorbers, and that is ascribed to higher absorption in the near-infrared part of the spectrum and size of gold sulfide core/gold shell nanoparticles. Higher increase of the temperature rate for capsules containing larger nanoparticles with enhanced absorption agrees with theoretical predictions, eq 4 and 5. We note that there are two main contributions to errors: the uncertainty from the temperature measurement and from the nonuniformity of the distribution of metal nanoparticles on capsules. The latter source is the predominant source of errors in the measurements. The data for temperature at the surface of capsules presented in Figure 6 were measured for up to five average looking capsules. From analysis of the temperature increase rates it can be concluded that the increased size, absorption, and surface density or surface filling factor resulted in a higher rate of the temperature increase. Practically, that leads to reduced surface densities of metal nanoparticles required for remote release of encapsulated materials. The remote release on capsules with core−shell nanoparticles was achieved with F_S under 0.05. The capsules with high surface filling factor were destroyed and buckled while those with lower surface filling factors were only slightly deformed. Higher temperature increase rate or higher efficiency of nanoparticles leads also to lower energy required for remote release. Therefore, development of novel metal nanoparticles with enhanced absorption in the near-infrared part of the spectrum, where the absorption of the tissue and cells is minimal, is essential for reducing intensities and concentration of nanoparticles.

In conclusion, we have presented the results of the influence of metal nanoparticles on the laser assisted remote release of encapsulated materials. The real-time remote release of encapsulated fluorescently labeled polymers from nanoengineered polyelectrolyte multilayer capsules is demonstrated by individually addressing a single capsule. The fluorescence signal from the rhodamine label of the polymer showed that all encapsulated polymer left the interior of the capsule after the release. It is shown that the release is possible from capsules with a low surface filling factor or surface density of metal nanoparticles and that the capsule does not need to be destroyed for the release to take place. Increasing the surface density of metal nanoparticles or their size and absorption results in increased damage and buckling of the capsules. An analytical model was introduced to investigate the influence of absorption, size, and surface density of metal nanoparticles on remote release. The model was tested both experimentally, by measuring the temperature rise in the vicinity of capsules, and numerically, by simulating the temperature distribution. Gold sulfide core/gold shell nanoparticles were found to be more efficient absorbing centers due to their larger size and increased near-infrared absorption. With incident laser light intensities of up to 50 mW, the temperature rise in the vicinity of the capsule can reach up to tens of degrees at higher surface densities, absorption, or size of nanoparticles. The results of the analysis presented in this work are relevant for studying the interaction of objects containing metal nanoparticles with external fields and can be used for further optimization of the materials and geometry parameters. The methods and technology presented in this work are of interest to drug delivery, specifically to the delivery of the medicine into biological cells.

Acknowledgment. We thank Rona Pitschke and Karen Köhler for TEM imaging and Michelle Prevot for SEM measurements. We kindly acknowledge the support by the 6th FP EU-project STREP001428 "Nanocapsules for targeted delivery of chemicals" and Volkswagen Foundation (I/80 051-054). We also thank the Sofja Kovalevskaya Program of the Alexander von Humboldt Foundation and the Emmy

Noether Program of the Deutsche Forschungsgemeinschaft (D.B., W.J.P.) for support.

Supporting Information Available: A movie in .avi format is available. This material is available free of charge via the Internet at http://pubs.acs.org.

References

(1) Möhwald, H.; Donath, E.; Sukhorukov, G. B. "Smart Capsules" in *Multilayer Thin Films. Sequential* Assembly of Nanocomposite Materials; Decher, G.; Schlenoff, J. B., Ed. Wiley-VCH: Weinheim, 2002.
(2) Donath, E.; Sukhorukov, G. B.; Caruso, F.; Davies, S. A.; Möhwald, H. *Angew. Chem., Int. Ed. Engl.* **1998**, *37*, 2202.
(3) Decher, G. *Science* **1997**, *277*, 1232.
(4) Sukhorukov, G. B.; Donath, E.; Lichtenfeld, H.; Knippel, E.; Knippel, M.; Budde, A.; Möhwald, H. *Colloids Surf. A* **1998**, *137*, 253.
(5) Sukhorukov, G. B.; Rogach, A. L.; Zebli, B.; Liedl, T.; Skirtach, A. G.; Köhler, K.; Antipov, A. A.; Gaponik, N.; Susha, A. S.; Winterhalter, M.; Parak, W. *Small* **2005**, *1*, 194.
(6) Ai, H.; Jones, S. A.; de Villiers, M. M.; Lvov, Y. M. *J. Controlled Release* **2003**, *86*, 59.
(7) Sershen, S. R.; Westcott, S. L.; Halas, N. J.; West, J. L. *J. Biomed. Mater. Res.* **2000**, *51*, 293.
(8) Skirtach, A. G.; Antipov, A. A.; Shchukin, D. G.; Sukhorukov, G. B. *Langmuir* **2004**, *20*, 6988.
(9) Sershen, S. R.; Westcott, S. L.; West, J. L.; Halas, N. *J. Appl. Phys. B* **2001**, *73*, 379.
(10) Radt, B.; Smith, T. A.; Caruso, F. *Adv. Mater.* **2004**, *16*, 2184.
(11) Antipov, A. A.; Sukhorukov, G. B.; Fedutik, Y. A.; Hartmann, J.; Giersig, M.; Möhwald, H. *Langmuir* **2002**, *18*, 6687.
(12) Dejugnat, C.; Sukhorukov, G. B. Stimuli-responsive Polyelectrolyte Microcapsules, in *Responsive Polymer Materials: Design and Applications*; Minko, S., Ed.; Blackwell Professional: Ames, IA, in press 2005.
(13) Dejugnat, C.; Sukhorukov, G. B. *Langmuir* **2004**, *20*, 7265.
(14) *Multilayer Thin Films. Sequential Assembly of Nanocomposite Materials*; Decher, G.; Schlenoff, J. B., Ed. Wiley-VCH: Weinheim, 2002.
(15) Shiratori, S. S.; Rubner, M. F. *Macromolecules* **2000**, *33*, 4213.
(16) Sukhishvili, S. A.; Granick, S. *J. Chem. Phys.* **1998**, *109*, 6861.
(17) Dähne, L.; Leporatti, S.; Donath, E.; Möhwald H. *J. Am. Chem. Soc.* **2001**, *123*, 5431.
(18) Rmaile, H. H.; Farhat, T. R.; Schlenoff, J. B. *J. Phys. Chem. B* **2003**, *107*, 14401.
(19) Dejugnat, C.; Halozan, D.; Sukhorukov, G. B. *Micromol. Rapid Commun.* **2005**, *26*, 961.
(20) Alivisatos, A. P.; Johnsson, K. P.; Peng, X.; Wilson, T. E.; Loweth, C. J.; Bruchez, M. P., Jr.; Schultz, P. G. *Nature* **1996**, *382*, 609.
(21) Schroedter, A.; Weller, H. *Angew. Chem., Int. Ed.* **2002**, *41*, 3218.
(22) Schmitt, J.; Maechtle, P.; Eck, D.; Möhwald, H.; Helm, C. A. *Langmuir* **1999**, *15*, 3256.
(23) Malikova, N.; Pastoriza-Santos, I.; Schierhorn, M.; Kotov, N.; Liz-Marzan L. M. *Langmuir* **2002**, *18*, 3694.
(24) Caruso, F.; Spasova, M.; Salgueirino-Maceira, V.; Liz-Marzan, L. M. *Adv. Mater.* **2001**, *13*, 1090.
(25) Corbierre, M.; Cameron, N.; Sutton, M.; Mochrie, S. G. J.; Lurio, L. B.; Ruhm, A.; Lennox, R. B. *J. Am. Chem. Soc.* **2001**, *123*, 10411.
(26) Lee, D.; Rubner, M. F.; Cohen, R. E. *Chem. Mater.* **2005**, *17*, 1099.
(27) Zhou, H. S.; Honma, I.; Komiyama, H.; Haus, J. W. *Phys. Rev. B* **1994**, *50*, 12052.
(28) Averitt, R. D.; Sarkar, D.; Halas, N. J. *Phys. Rev. Lett.* **1997**, *78*, 4217.
(29) Norman, T., Jr.; Grant, C. D.; Magana, D.; Zhang, J. Z.; Liu, J.; Cao, D.; Bridges, F.; van Buuren, A. *J. Phys. Chem. B* **2002**, *106*, 7005.
(30) Raschke, G.; Broglk, S.; Susha, A. S.; Rogach, A. L.; Klar, T. A.; Feldmann, J.; Fieres, B.; Petkov, N.; Bein, T.; Nichtl, A.; Kuerzinger, K. *Nano Lett.* **2004**, *4*, 1853.
(31) Zhang, J. Z.; Schwartzberg, A. M.; Norman, T. Jr.; Grant, C. D.; Liu, J.; Bridges, F.; van Buuren, T. *Nano Lett* **2005**, *5*, 809.
(32) Raschke, G.; Broglk, S.; Susha, A. S.; Rogach, A. L.; Klar, T. A.; Feldmann, J.; Fieres, B.; Petkov, N.; Bein, T.; Nichtl, A.; Kuerzinger, K. *Nano Lett.* **2005**, *5*, 811.
(33) Goldenberg, H.; Tranter, C. J. *Brit. J. Appl. Phys.* **1952**, *3*, 296.
(34) Lax, M. *J. Appl. Phys.* **1977**, *48*, 3919.
(35) Pitsillides, C. M.; Joe, E. K.; Wei, X.; Anderson, R. R.; Lin, C. *Biophys. J.* **2003**, *84*, 4023.
(36) Braun, D.; Libchaber, A. *Phys. Rev. Lett.* **2002**, *89*, 188103.
(37) Duhr, S.; Arduini, S.; Braun, D. *Europ. Phys. J. E* **2004**, *15*, 277.
(38) Temperature values were obtained taking into consideration thermophoresis of the dye with Soret coefficient of 0.015/K. Half of the change of the dye's intensity is due to the pH drop and half due to thermophoresis, resulting in a sensitivity of the dye of 1.85% fluorescence change per degree K when measuring small temperature changes near 20 °C.
(39) Gittins, D. I.; Susha, A. S.; Schoeler, B.; Caruso, F. *Adv. Mater.* **2002**, *14*, 508.
(40) Kreibig, U.; Vollmer, M. In *Optical Properties of Metal Clusters*; Springer-Verlag: Berlin, 1995.

NL050693N